Application of transient CHI plasma startup to future ST and AT devices

Cite as: Phys. Plasmas **26**, 032501 (2019); https://doi.org/10.1063/1.5087259
Submitted: 30 December 2018 . Accepted: 07 February 2019 . Published Online: 01 March 2019

K. C. Hammond, R. Raman, and S. C. Jardin

Physics of Plasmas ARTICLE scitation.org/journal/php

Application of transient CHI plasma startup to future ST and AT devices

Cite as: Phys. Plasmas **26**, 032501 (2019); doi: 10.1063/1.5087259
Submitted: 30 December 2018 · Accepted: 7 February 2019 ·
Published Online: 1 March 2019

K. C. Hammond,[1,a)] R. Raman,[2,b)] and S. C. Jardin[3]

AFFILIATIONS

[1]Max Planck Institute for Plasma Physics, 17491 Greifswald, Germany
[2]University of Washington, Seattle, Washington 98195, USA
[3]Princeton Plasma Physics Laboratory, Princeton, New Jersey 08450, USA

This paper is part of the Special Collection Papers from the 60th Annual Meeting of the APS Division of Plasma Physics.
Note: Paper TI2 6, Bull. Am. Phys. Soc. **63** (2018).
[a)]Invited speaker.
[b)]raman@aa.washington.edu

ABSTRACT

Employment of non-inductive plasma start-up techniques would considerably simplify the design of a spherical tokamak fusion reactor. Transient coaxial helicity injection (CHI) is a promising method, expected to scale favorably to next-step reactors. However, the implications of reactor-relevant parameters on the initial breakdown phase for CHI have not yet been considered. Here, we evaluate CHI breakdown in reactor-like configurations using an extension of the Townsend avalanche theory. We find that a CHI electrode concept in which the outer vessel wall is biased to achieve breakdown, while previously successful on NSTX and HIT-II, may exhibit a severe weakness when scaled up to a reactor. On the other hand, concepts which employ localized biasing electrodes such as those used in QUEST would avoid this issue. Assuming that breakdown can be successfully attained, we then apply scaling relationships to predict plasma parameters attainable in the transient CHI discharge. Assuming the use of 1 Wb of injector flux, we find that plasma currents of 1 MA should be achievable. Furthermore, these plasmas are expected to Ohmically self-heat with more than 1 MW of power as they decay, facilitating efficient hand-off to steady-state heating sources. These optimistic scalings are supported by Tokamak Simulation Code simulations.

I. INTRODUCTION

The ability to operate a tokamak without a central solenoid would greatly ease the engineering constraints on the design of tokamak-based fusion reactors. In particular, it would allow more space within the central column for a tritium blanket. In a spherical tokamak (ST) device, this would make it easier to attain the required low aspect ratio.

In the absence of a solenoid, however, alternate means must be developed in order to start up the plasma and generate a toroidal current. To this end, a number of strategies have been explored to date.[1] One example would be to generate a loop voltage by ramping the poloidal field (PF) coils.[2,3] Other possibilities involve the use of radio-frequency (RF) heating and current drive, particularly at lower-hybrid and electron-cyclotron frequencies.[4,5]

A third approach involves helicity injection, in which a closed-flux toroidal plasma is formed from discharges created between electrodes located on the periphery. These electrodes could take the form of plasma guns, as is the case in local, or point-source helicity injection,[6] or biased rings extending around the torus, in the case of coaxial helicity injection (CHI).[7]

The helicity injection may occur on a steady-state or transient basis. In the former case, current is continuously applied between the bias electrodes, and plasma from the electrode discharge is transferred to the closed-flux toroidal plasma through reconnection induced by three-dimensional magnetic perturbations. In the latter case, a short, high-current burst of plasma is generated between the electrodes, leading to the formation of a transient closed-flux toroidal plasma via a predominantly two-dimensional reconnection process.[8–10] Once a transient CHI discharge is created, it may be subsequently developed and maintained by steady-state heating sources such as neutral beam injection (NBI) or electron-cyclotron resonance heating (ECRH).

In principle, steady-state CHI techniques can sustain a toroidal plasma with closed flux surfaces indefinitely. In experiments conducted to date, however, steady-state CHI plasmas are typically

unsuccessful in burning through the low-charge-state impurities that are continuously released due to the interaction of the plasma with the biasing electrodes. Partly due to this effect, good confinement—in the sense of the L/R decay time of the plasma if the current source is removed—has not been demonstrated in actively driven plasmas. Experiments with transient CHI, on the other hand, have succeeded in attaining closed-flux plasmas with toroidal currents of 100 kA or greater and temperatures of 30–50 eV which can persist for tens of ms without additional power input after the bias is shut off.[11,12] A further advantage of transient CHI is that its scaling with the device size and the magnetic field is robust and well understood,[13] and the scaling relationships predict substantially improved performance capability in larger devices with higher fields.

The first step of any transient CHI discharge is the initial breakdown of the plasma, which occurs with the formation of a Townsend avalanche[14] between the biased electrodes upon the release of working gas. To date, no detailed predictive modeling of the plasma breakdown has been carried out for reactor-scale configurations. However, this phase must be taken into account, as the parameters which govern breakdown are not exactly the same as those which determine the ultimate performance of the CHI discharge—and in some cases, the criteria are at odds with one another.

In this paper, we study the requirements for plasma breakdown in reactor-scale configurations. Ultimately, our findings indicate that transient CHI can be a highly capable solenoid-free startup technique, provided certain pitfalls are avoided in the design of the bias electrodes.

In Sec. II, we consider the plasma breakdown requirements for two different concepts for biasing electrodes. The first concept, which was employed successfully in NSTX and HIT-II, biases the entire outboard first side of the first wall relative to the inboard side. The second biases a ring electrode, located in the divertor and extending toroidally around the vessel, relative to the nearby first wall. We find that the first concept is vulnerable to breakdown in undesired parts of the vessel if it is implemented in a reactor with larger dimensions and a stronger magnetic field, potentially preventing the attainment of transient CHI discharges. On the other hand, the concept which uses a localized ring electrode avoids the problem altogether. In Sec. III, we employ CHI scaling relationships to predict the achievable parameters in transient CHI discharges in reactor-scale devices, and find that it should be possible to achieve plasmas with up to 1 MA of closed-flux toroidal current and with Ohmic self-heating powers of more than 1 MW. Finally, in Sec. IV, we show the results of simulations with the **T**okamak **S**imulation **C**ode (TSC) which support the scaling relationships assumed for the predictions made in Sec. III.

II. CHI BREAKDOWN IN REACTOR-SCALE DEVICES

The reactor designs considered in this paper are based on a concept for a **S**pherical **T**okamak-based **F**usion **N**uclear **S**cience **F**acility (ST-FNSF) designed by Brown *et al.*[15] An overview of the concept is shown in Fig. 1(a). The design includes space for a neutron blanket and enables a number of advanced tokamak features including a Super-X divertor. The design also incorporates numerous divertor PF coils which are advantageous for both implementing Super-X magnetic configurations and generating high levels of the injector flux, the latter of which is advantageous for CHI applications.

The two bias electrode concepts considered here are shown in Figs. 1(b) and 1(c). In the first concept [Fig. 1(b)], the entire outer first wall is biased relative to the inner first wall. This concept was implemented in both HIT-II[16] and NSTX,[7] and hereafter will be referred to as the "NSTX-like" concept. In this case, the inner and outer walls are electrically isolated from one another on both the top and the bottom of the vessel. In the second concept [Fig. 1(c)], a toroidally extending ring localized at the divertor area is biased relative to the entire first wall. This concept resembles a divertor ring electrode that was implemented for some time in DIII-D[17] and hereafter will be referred to as the "DIII-D-like" configuration. The ring electrode is assumed to be isolated from the adjacent wall with a continuous dielectric plate with no vacuum gaps; hence, breakdown can only occur between the electrode and the opposing wall. Breakdown along the edges of the insulator wall can be controlled as described at the end of this section.

Details on how the electrical isolation can be implemented in the reactor for both cases, as well as methods for shielding the isolators from neutron radiation, are given in Ref. 18. For the DIII-D-like configuration, we will note that whereas we show the biased electrode in the lower divertor region, the electrode is positioned at the upper divertor in Ref. 18 (Fig. 4). We chose the lower divertor region for this study largely because this has been the location of the injector current in previous CHI experiments, and from the perspective of plasma breakdown and start-up, it does not matter whether the electrode is in the upper or lower divertor. In a reactor, however, the upper divertor region is more suitable. The electrode then sits on top of the toroidal insulator plate, which in turn rests on top of the outer blanket structure. Both the electrode and the insulator are thus primarily supported by gravity. Also, as shown in Ref. 18, at this location, the insulator is well shielded from neutrons by the blanket structure located below the insulator. We note that the CHI system on the new URANIA device at the University of Wisconsin is planned to be installed in the upper divertor.

When evaluating the breakdown requirements for CHI electrode configurations, it is important not just to determine the necessary parameters to achieve breakdown but also to ensure that the discharge will form in the desired location. Hence, we will evaluate the breakdown for these configurations using the spatially resolved approach developed in Ref. 19, which applies the Townsend avalanche theory to individual flux tubes linking the two electrodes.

Within a given flux tube, the critical parameters for breakdown are the field line connection length L_c between the two electrodes, the working gas pressure p, and the parallel electric field $E_\parallel$. In the case of CHI, the integral of $E_\parallel$ along the flux tubes connecting opposite electrodes is equal to the applied bias V. Also important are the two Townsend coefficients A and B, which depend on the gas species used. For deuterium, $A = 510\ \mathrm{m^{-1}\,Torr^{-1}}$ and $B = 1.25 \times 10^4\ \mathrm{V\,m^{-1}\,Torr^{-1}}$.[20]

A key prediction of the avalanche theory is the minimum electrode bias V_{bd} to initiate the breakdown of a gas[14]

$$V_{bd} = \frac{BL_c p}{\ln(AL_c p) - \ln[\ln(1 + 1/\gamma)]}. \quad (1)$$

This is the well-known equation for the Paschen curve for breakdown between two parallel plates,[14] and a schematic plot is shown in Fig. 2. Here, γ is the secondary electron emission coefficient, equal to the number of electrons produced per impact ionization during the avalanche, due to processes other than impact ionization. One such

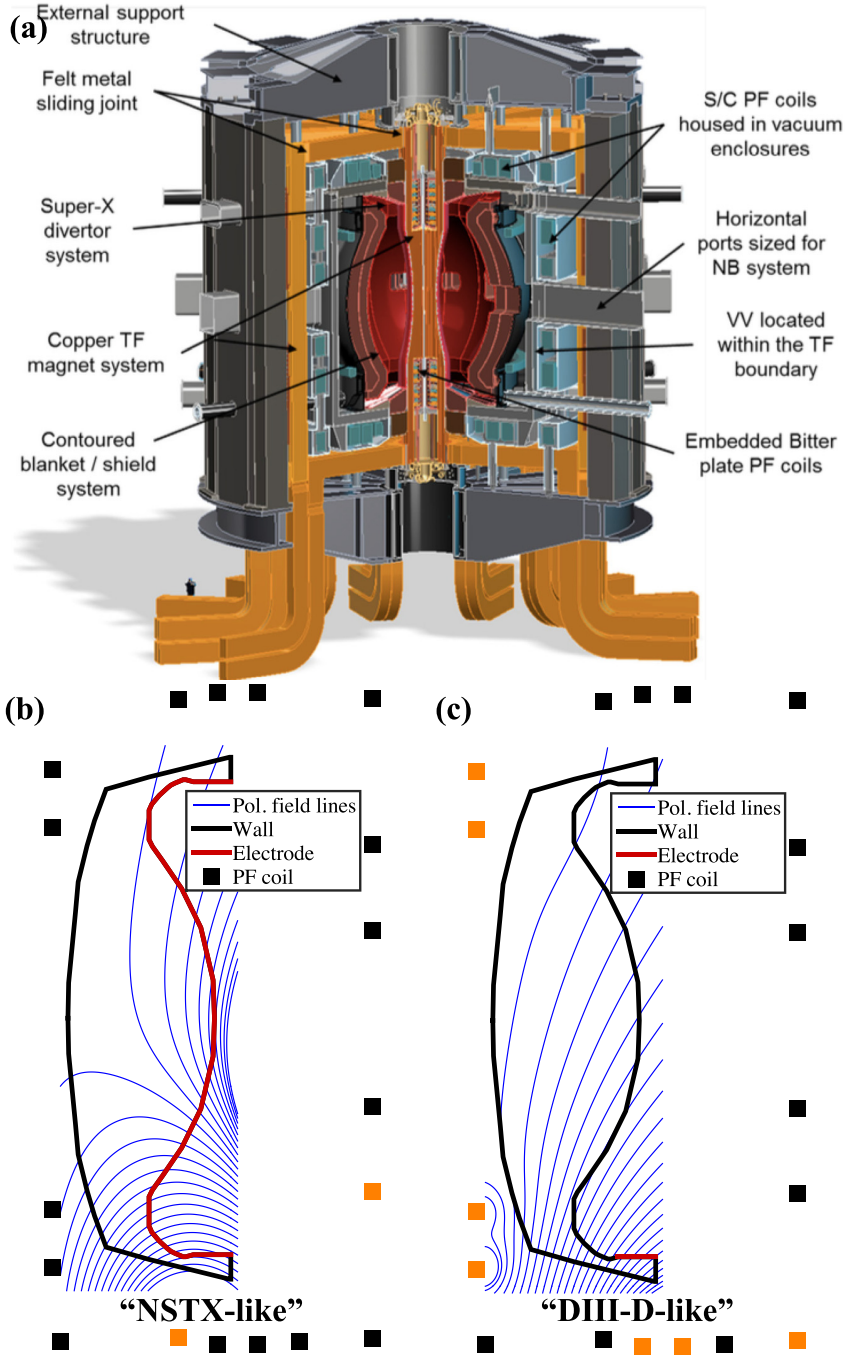

FIG. 1. (a) Overview of the conceptual design for a ST-FNSF reactor as designed by Brown and Menard. Reproduced with permission from Brown *et al.*, Fusion Sci. Technol. **68**, 277 (2015). Copyright 2015 Taylor & Francis Ltd. (b) Poloidal cross-section showing the first wall and the locations of the poloidal field coils. In the "NSTX-like" electrode configuration, the red portion of the first wall is biased relative to the black portion. Active poloidal field coils for this configuration are shown in orange. Poloidal projections of the resulting field lines are shown in blue. (c) Similar poloidal cross-section, indicating the electrode geometry for the "DIII-D-like" configuration where the biased electrode is localized to the divertor area.

process, as the name suggests, is secondary emission of electrons upon ion impact on the anode plate.

This model has been applied to Ohmic heating in tokamaks by interpreting V_{bd} as the integral of the parallel electric field $E_{\|}$ induced by the central solenoid along the length of the flux tube.[21] Good agreement between the model and experiment for Ohmic start-up has been found for $\gamma = 0.58$.[19,21–23] Note that, with γ fixed at 0.58, the second term in the denominator of Eq. (1) vanishes. Hence, the condition in Eq. (1) for Ohmic breakdown has often been expressed by dividing both sides by L_c to yield, approximately, $E_{\|,bd} = Bp/\ln(AL_cp)$. For the rest of this section, we will also adopt the assumption $\gamma = 0.58$.

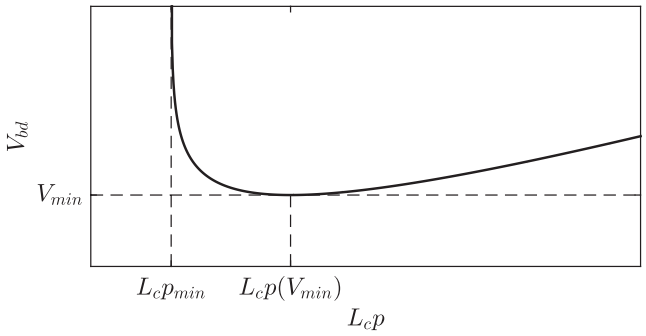

FIG. 2. Schematic of the Paschen curve, relating the required electrode voltage for breakdown V_{bd} to the product of connection length L_c and gas pressure p [Eq. (1)]. Both axes have logarithmic scales. The locations of key quantities considered in this paper (V_{min}, p_{min}, and $p(V_{min})$) are also shown.

From the denominator of Eq. (1), it is clear that, for a given connection length L_c, breakdown cannot occur at pressures less than or equal to

$$p_{min} \equiv \frac{1}{AL_c} \ln(1 + 1/\gamma) \tag{2}$$

at any bias voltage. This corresponds to the vertical asymptote of the Paschen curve (Fig. 2). The connection length L_c is dependent on the vessel geometry and the magnetic field line trajectories and scales roughly as aB_t/B_p, where B_t is the toroidal component of the magnetic field, B_p is the poloidal component, and a is the distance between the vessel walls along the poloidal field component.[21]

As a baseline scenario for both electrode configurations, a toroidal field of $B = 3$ T on the axis at a major radius $R = 1.7$ m will be assumed. Furthermore, the PF coils will be used to generate approximately 1 Wb of poloidal flux ψ_{inj} through the injector electrodes. This is 20 times the level used for CHI experiments in NSTX.[1] For the transient CHI start-up, higher levels of ψ_{inj} are generally advantageous because the amount of closed-flux toroidal current I_p that can be generated with transient CHI is directly proportional to ψ_{inj}.[1,13] It is possible to employ greater ψ_{inj} (i.e., higher B_p) on the reactor scale, because B_t and a are also greater. Both of these factors compensate for the reduction in L_c (and subsequently higher p_{min}) that would otherwise result from an increase in the poloidal field.

The values of the minimum breakdown pressure at different locations within the plasma vessel are plotted in Fig. 3 for the two electrode configurations. Here, each flux tube is parameterized by the radial r and vertical z coordinates at which it intersects the poloidal plane, such that p_{min} (r, z) can be represented as contours in this plane. Regions where breakdown cannot occur—as a result of the flux tubes not connecting opposite bias electrodes—are shown in white.

In both configurations, the breakdown must occur in the lower portion of the vessel or in the lower divertor, where the spacing between the electrodes is relatively narrow, to enable an efficient conversion of ψ_{inj} to closed poloidal flux ψ_{pol}. Indeed, the predictions for p_{min} in both configurations indicate that breakdown should be possible in the lower divertor area at pressures of 10^{-4} to 10^{-3} Torr.

However, note that in the main vessel area in the NSTX-like electrode configuration [Fig. 3(a)], p_{min} is 3–4 orders of magnitude lower

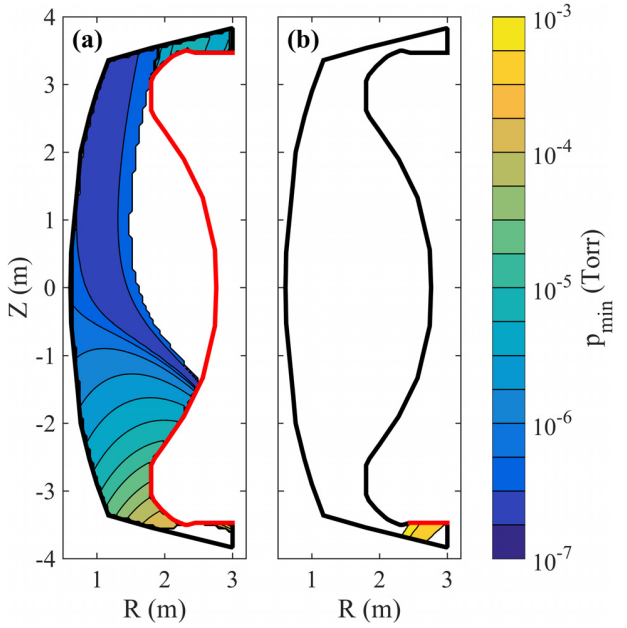

FIG. 3. Contours of the minimum pressure p_{min} (r, z) [Eq. (2)] required for plasma breakdown within the poloidal vessel cross-section for (a) the NSTX-like electrode configuration and (b) the DIII-D-like electrode configuration. Portions of the wall which constitute the biased electrode for each configuration are shown in red. Regions where breakdown could not occur at any pressure (due to the local flux tube not connecting opposite electrodes) appear as white.

than in the lower divertor area. In fact, the predicted levels on the order of 10^{-7} Torr may not be much greater than the base pressure of a fusion device.

Under these conditions, it would be difficult to ensure that breakdown occurs near the lower divertor, rather than in the middle of the vessel. To attain the higher pressures necessary for breakdown in the desired area, working gas would be fed quickly into the lower divertor area after the bias voltage is applied to the plates, ideally causing the gas to break down near the bottom of the vessel before it spreads to the rest of the chamber. But, since p_{min} in the main vessel is so much lower than in the lower divertor, there is a high risk that enough gas would leak into the main vessel to cause breakdown there before it can occur in the lower divertor, resulting in a failure of the transient CHI discharge.

This failure mode was occasionally observed in NSTX, where a similar electrode configuration was employed, as shown in Fig. 4 of Ref. 19. However, due to the smaller vessel size and the lower toroidal field employed, the connection lengths in the main NSTX vessel were at least one order of magnitude lower, resulting in correspondingly higher values of p_{min}. Thus, while the issue was relatively easy to avoid in NSTX, it would become increasingly difficult as the device size and the toroidal field increase.

We note that there are a number of factors that could mitigate this failure mode. One example is derived simply from the larger dimensions of the ST-FNSF device relative to NSTX. While the larger dimensions, on the one hand, contribute to greater L_c, they will, on the other hand, increase the amount of time required for the gas to leak

from the divertor area from the main vessel. Thus, through good control of the gas injection to the desired breakdown location, breakdown in the rest of the vessel could in principle be suppressed. But the primary factor that makes this more challenging for large machines is that the required pressures for breakdown in the main vessel are just too close to the vacuum base pressure.

It is therefore not recommended to use this electrode configuration for transient CHI in a fusion device. Instead, at least one of the CHI electrodes should be a poloidally localized toroidal ring. As seen in Fig. 3(b), this configuration permits for the region where breakdown is possible to be restricted to the desired area. Under these circumstances, the risk of undesired breakdown in the main vessel is eliminated, and there would be no need for the development of mitigation strategies.

One additional aspect that must be considered for a configuration involving a biased ring electrode is that the discharge could occur between the electrode and the metal structure that supports the insulator. Indeed, during the biased electrode design for QUEST,[24] this was an issue of concern. However, transient CHI (in comparison to steady-state CHI) has one important advantage that permits electrode configurations such as this. During the transient CHI start-up, there is no pre-existing plasma, which allows one to provide an initial magnetic configuration [as shown, for example, in Fig. 1(c)] and gas injection conditions that are advantageous for initiating the discharge at the desired location. Thus, for instance, on QUEST, the initial vacuum injector flux is programmed to connect the electrode plate to the opposite wall. Field lines that connect the electrode to the wall supporting the insulator are minimized. Finally, the gas necessary for discharge initiation is directed from the ground electrode directly onto the high-voltage electrode. These conditions make it highly probable for the discharge to form in the desired location. In transient CHI, as the voltage is rapidly reduced after the start of the primary discharge, it becomes much more difficult for the discharge to start at other locations. The results from QUEST were able to show that spurious arcing at other locations could be completely suppressed by appropriate programming of the injector flux and gas conditions. So, initiating the discharge in the desired location should be achievable in ST-FNSF configurations as well.

III. PROJECTIONS FOR ATTAINABLE PARAMETERS IN TRANSIENT CHI DISCHARGES

In this section, we will consider only the DIII-D-like electrode configuration and make predictions on attainable plasma parameters and associated experimental requirements under the assumption of $\psi_{inj} = 1$ Wb. Even higher levels of ψ_{inj} should be attainable in this device, thanks to the abundance of PF coils located near the divertor (Fig. 1); however, only 1 Wb will be considered for this study.

Four different variants of the ST-FNSF concept will be considered. The first, labeled ST-3, uses the nominal vessel geometry and the magnetic field as described in Sec. II. The second variant, labeled ST-6, will assume the same vessel geometry, but twice the field (i.e., $B_0 = 6$ T on axis). The next two configurations will be "advanced-tokamak" devices with the same cross-sectional geometry as the ST configurations, but with all radial coordinates displaced outward by 0.7 m. They will be labeled AT-6 and AT-9 with on-axis toroidal fields $B_0 = 6$ T and $B_0 = 9$ T, respectively.

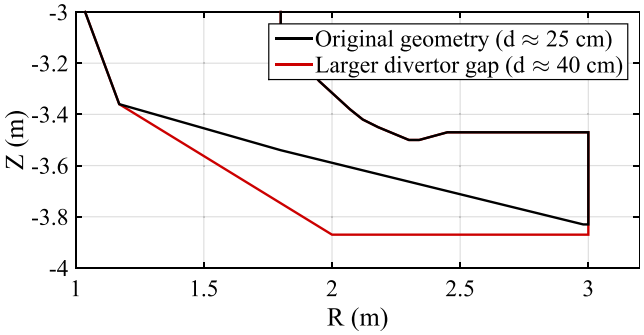

FIG. 4. Comparison of the two variants of the bias electrode geometry used for the analysis in Sec. III.

For each of these configurations, two variants of the electrode geometry will be assessed. These variants are shown in Fig. 4. The first has the original geometry of the Brown-Menard design, which has approximately $d = 25$ cm of separation between the biased electrode and the magnetically connected portion of the counter-electrode (vessel wall). The second is modified to have a greater spacing ($d = 40$ cm) between the biased and counter-electrodes. The larger gap in this modified design would ease the requirements both for breakdown and for CHI injection, as will be shown in Secs. III A and III B.

Selected requirements and predicted transient CHI plasma parameters for these configurations are listed in Table I. The quantities therein will now be described in more detail.

A. Breakdown requirements

For a given magnetic configuration and vessel geometry, the main parameters of interest for attaining initial breakdown between the CHI electrodes are the electrode bias V and gas pressure p. The former parameter partly determines requirements on the capacitor bank used to charge the electrodes and supply the injector current. The latter determines the amount of gas that must be injected in order to attain breakdown. In general, the more the initial working gas is

TABLE I. Required input parameters and predicted attainable plasma parameters for the four variants of the FNSF configuration considered in this paper.

Parameter	Dimension	ST-3	ST-3	ST-6	ST-6	AT-6	AT-6	AT-9	AT-9
ψ_{inj}	Wb	1	1	1	1	1	1	1	1
R_{maj}	m	1.7	1.7	1.7	1.7	2.4	2.4	2.4	2.4
B_0	T	3	3	6	6	6	6	9	9
d	cm	25	40	25	40	25	40	25	40
V_{min}	V	310	310	310	310	310	310	310	310
$p(V_{min})$	mTorr	6.3	4.2	3.2	2.1	2.3	1.5	1.5	1
I_{PF}	kA	780	780	780	780	610	610	610	610
I_{inj}	kA	790	310	400	160	280	110	190	73
n_{plasma}	10^{17} m^{-3}	56	60	28	30	18	19	12	12
I_p	MA	1.1	1.1	1.1	1.1	0.77	0.77	0.77	0.77
P_{self}	MW	3.8	3.8	3.8	3.8	2.7	2.7	2.7	2.7
n_{O1}	10^{17} m^{-3}	870	870	3500	3500	3500	3500	7900	7900

injected, the lower the final temperature of the CHI discharge will be if the injected energy remains the same. This implies that a higher initial pressure requirement will tend to make it more difficult to attain a transient CHI discharge that can burn through its low-charge-state impurities and be efficiently handed off to steady-state heating sources.

From Eq. (1), it follows that the product $L_c\,p$ can be optimized to minimize the necessary bias voltage to attain breakdown. For a given L_c, the optimal pressure is

$$p(V_{\min}) = \frac{\exp(1)}{AL_c}\ln(1+1/\gamma). \tag{3}$$

This corresponds to the minimum of the Paschen curve shown in Fig. 2.

For the analysis in this section, we will use a different value of γ from the value of 0.58 assumed in Sec. II, since the primary region of concern here is the lower divertor area rather than the main vessel. It was postulated in Ref. 19 that the assumption $\gamma = 0.58$ works well for regions in the main vessel where flux tubes make many toroidal revolutions, whereas a lower estimate may be necessary for the divertor area where flux tubes may make less than one revolution. Considering that $\gamma \approx 0.05$ has been observed for deuterium discharges between parallel plates,[25] we will make the conservative assumption that $\gamma = 0.01$.

In further calculations which rely on $p(V_{\min})$, the median value within the region between the electrodes (where breakdown is possible) will be used for each configuration. This value is also shown in Table I, and ranges from 6 mTorr in the ST-3 case with the as-designed electrode geometry to 1 mTorr in the AT-9 case with the wider electrode gap. The downward trend in $p(V_{\min})$ with increasing electrode gap spacing, aspect ratio, and toroidal field is due to the fact that all of these changes result in longer connection lengths L_c between the electrodes.

The optimal breakdown voltage $V_{\min}$ is

$$V_{\min} = \frac{B}{A}\exp(1)\ln(1+1/\gamma), \tag{4}$$

which is 310 V for deuterium with $\gamma = 0.01$. Capacitor banks can easily exceed this value, so it should not be a problem to supply sufficient voltage for breakdown.

B. Transient CHI requirements

The target injector flux ψ_{inj} of 1 Wb will result in more strenuous input parameters compared to earlier experiments. Producing this amount of flux through the electrodes will require PF coil currents up to 800 kA. The relative proximity of the PF coils to the plasma in the FNSF configurations considered here permits the attainment of 1 Wb without any of the PF coil currents needing to exceed 1 MA.

The main affected requirement is the amount of injector current I_{inj} which the electrodes must reach or exceed for the initial plasma to expand into the main vessel. This is derived from a simple model (the bubble burst model) that balances the magnetic field line tension in coaxial geometry with the $j \times B$ force needed to overcome the tension. As described in Eq. (2) of Ref. 13, the relevant equation in cylindrical geometry is

$$I_{\text{inj}} B_t d = \frac{2\pi a d B_z^2}{2\mu_0}, \tag{5}$$

where B_t is the average toroidal field between the electrodes, d is the spacing between the coaxial electrodes, and a is the average radius of the two electrodes. The term on the right is the force required to stretch the radial injector flux and B_z is the magnetic field that results from the radial injector flux being stretched inside the electrode gap region. The term on the left is the applied axial force that results from the current flowing between the electrodes, and it is analogous to the *IBL* force acting on an armature in a simple rail gun geometry.

Applying Ampère's law to rewrite B_t as $\mu_0 I_{\text{TF}}/2\pi a$, where I_{TF} is the total current in the toroidal field coils, and noting that the injector flux $\psi_{\text{inj}} = \pi a d B_z$, the minimum injector current may be expressed as (Eq. (3) in Ref. 13)

$$I_{\text{inj}} = \frac{2\psi_{\text{inj}}^2}{\mu_0^2 d^2 I_{\text{TF}}}. \tag{6}$$

We note that a more detailed study using the TSC code[26] was able to show consistency with this simple relation.

In practice, the injector current will rarely exceed this value due to the increase in the impedance of the plasma between the injectors once it expands into the vessel.[1] This value ranges from 790 kA for the ST-3 configuration with as-designed electrode geometry down to 73 kA for AT-9 with the wider gap. As can be seen from Eq. (6) and Table I, a higher toroidal field and a wider electrode gap will ease the demands on the injector power supply for all configurations.

C. Expected plasma parameters

The density n_{plasma} of the transient CHI plasma will be estimated from $p(V_{\min})$. We will assume that the total amount of gas released into the injector area will be just enough to fill the lower divertor area, a toroidal cavity with a radial width of 55 cm and a height of $d = 25$ cm or 40 cm depending on the electrode gap width. This gas inventory will further be assumed to fully ionize and form a plasma which essentially fills the main vessel, leading to the estimate for the plasma density, n_{plasma}. In all configurations considered here, the density is expected to be below 10^{19} m^{-3} (Table I). Unlike $p(V_{\min})$ and I_{inj}, n_{plasma} does not depend strongly on d, due to the fact that the lower required breakdown pressure for $d = 40$ cm is compensated by the larger volume of the gap itself in setting the requirement for total gas inventory.

The attainable closed-flux plasma current will be estimated as follows:[27]

$$I_{\text{p}} = \frac{2\psi_{\text{pol}}}{\mu_0 R l_i}. \tag{7}$$

Here, ψ_{pol} is the poloidal flux within the closed flux surfaces and l_i is the effective inductance of the injected CHI plasma. Reconstructions by the equilibrium fitting code EFIT[31] of transient CHI-initiated discharges in NSTX typically indicated that approximately 70% of the injector flux was converted to poloidal flux[27]

$$\psi_{\text{pol}} \approx 0.7\psi_{\text{inj}}. \tag{8}$$

Furthermore, the normalized inductance of these discharges was found to be 0.35. For a conservative estimate of the attainable plasma current, we will assume $l_i \approx 0.6$. Under these assumptions, I_{p} is expected to reach 1.1 MA for the ST variants and 0.77 MA for the AT variants.

The above estimates for I_p and n_{plasma} should be interpreted as peak values which the transient CHI plasma is expected to reach around the time the electrode biasing current is shut off. Subsequently, the plasma will, of course, decay in the absence of external heating. This decay process is expected to play a beneficial—and possibly, crucial—role in the plasma development. This is because the reduction in poloidal flux ψ_{pol} during the decay process will induce a loop voltage, causing the plasma to self-heat. The Ohmic self-heating will in turn raise the electron temperature, thereby improving the coupling efficiency to neutral beams and ECRH. The total heating power resulting from this process is as follows:

$$P_{self} = \frac{\Delta\psi_{pol}}{\tau} I_p. \quad (9)$$

The inductance of the plasma with ST-FNSF dimensions is expected to be $L = l_i R\mu_0/2 = 0.65\ \mu$H. For a 50 eV plasma with the ST-FNSF cross-section, the resistivity would be approximately 19 $\mu\Omega$, resulting in an L/R decay time τ of about 35 ms. At 100 eV, the L/R time increases by a factor of three. As will be shown in Sec. IV, using TSC simulations, τ will increase over time as the plasma heats up. For the calculation of P_{self}, we will choose $\tau = 200$ ms. This is conservative in this context as it reduces the induced loop voltage and the resulting Ohmic dissipation, and therefore the increase in the plasma temperature. Under these assumptions, values ranging from 2 to 4 MW are expected for each configuration.

Should the Ohmic self-heating power not be sufficient to attain sufficient temperatures for coupling with neutral beams, it should also be possible to supplement the self-heating process with ECRH. This is due to the fact that the expected plasma densities are all well below the cutoff densities for the first-harmonic O-mode ECRH (n_{O1}), here calculated assuming a heating frequency which would deposit energy on the magnetic axis.

Overall, the estimated parameters in Table I indicate that transient CHI start-up has strong potential as a solenoid-free start-up technique in reactors, indicating that MA-scale plasma currents should be attainable with feasible levels of PF coil current and injector current. Furthermore, plasma breakdown should be readily attainable without requiring the injection of an impractical amount of gas between the injectors. While the requirements are generally less stringent for configurations with higher toroidal fields, higher aspect ratios, and wider electrode gaps, there is good reason to expect transient CHI startup to succeed even in the ST-FNSF reactor with the 3 T field strength as currently envisioned.

IV. COMPARISON OF SCALING RELATIONSHIPS WITH TSC SIMULATIONS

The estimates for attainable plasma parameters in Sec. III relied on simple scaling relationships, which are generally favorable as the magnetic field and the device size increase. Furthermore, both the high values of plasma current and Ohmic self-heating power were derived assuming the use of high levels of injector flux which have no experimental precedent to date. It is therefore worthwhile to conduct more detailed modeling to verify the predicted impact of increases in injector flux on plasma current and self-heating power. In addition, through this modeling, we will be able to more quantitatively assess the electron temperature increases that could be realized with more poloidal flux injection.

To this end, we have employed the TSC. TSC is a time-dependent, free-boundary, predictive equilibrium evolution and transport code.[28,29] It has previously been used for the development of both discharge scenarios and plasma control systems. It solves fully dynamic MHD/Maxwell's equations coupled to transport and circuit equations. The device hardware, coil, and electrical power supply characteristics are provided as input. It models the evolution of a free-boundary axisymmetric toroidal plasma on the resistive and energy confinement time scales. The plasma equilibrium and field evolution equations are solved on a two-dimensional Cartesian grid. Boundary conditions between plasma/vacuum/conductors are based on the poloidal flux and tangential electric field being continuous across interfaces. The circuit equations are solved for all the poloidal field coil systems with the effects of induced currents in passive conductors included. Currents flowing in the plasma on open field lines are included, and the toroidally symmetric part of this "halo current" is computed.

For modeling CHI, the vacuum vessel is specified as a conducting structure with poloidal breaks at the location of the isolation gaps between the bias electrodes across which an electric potential difference is applied. From this, the TSC calculates the injector current using a model for the resistivity of the "halo" plasma. This circuit, however, contains a sheath resistance at each electrode, which is difficult to model. Since for the purposes of this study, it is the injector current and flux that are important, we adopted the modeling strategy of adjusting the injector voltage in order to attain the current required to evolve the injector flux into the vessel.

A. Simulation of CHI plasma evolution

TSC simulations of transient CHI discharges in NSTX have successfully demonstrated current persistance;[26] that is, the toroidal current persists after the injector current has been reduced to zero. This generation of closed flux is the result of an effective (positive) toroidal loop voltage induced by the changing poloidal flux on the open field lines as the injector current is reduced to zero.

The CHI discharge is initiated in TSC as described in Ref. 26, and continued until a suitable closed-flux target is established. The first step involves current driven by the external injector circuit on purely open field lines. After this discharge fills the vessel, the applied CHI voltage is rapidly reduced. The resulting decrease in the injector current, which also causes the injected poloidal flux to decrease, induces a positive loop voltage that causes the generation of closed field lines carrying toroidal current. At the onset of flux closure, a second step in the simulation is initiated. This continuously solves for the plasma boundary, including locating the divertor X-point, and begins solving the flux surface averaged transport equations. This phase begins 17 ms after the CHI discharge is first initiated. At 17 ms, horizontal position control is implemented to position and stabilize the CHI plasma. This is different from the conventional inductive start-up in which the early plasma is usually positioned on the center column, and the plasma is located much farther away from the equilibrium control coils than the CHI discharge is. Then, at 40 ms, vertical position control is used to vertically center the highly up-/down-asymmetric CHI plasma.

B. Effects of increased toroidal flux

For the simulations in this paper, we have used NSTX vessel geometry as simulated in Ref. 26, but have employed higher toroidal

fields and levels of injector flux. Hence, the results should not be interpreted as direct predictions for what to expect for the ST-FNSF configurations considered in Sec. III; rather, they are simply meant to illustrate the impact of increasing the injector flux while holding other parameters constant.

For these simulations, the initial electron temperature for the CHI discharge is 50 eV. This is a reasonable starting value based on the present observations of approximately 30 eV electron temperatures achieved on NSTX CHI discharges and even higher temperatures on the HIT-II experiment. During the transient CHI start-up, low-Z impurities are the primary source of energy loss, and both NSTX and HIT-II used graphite electrodes for the cathode. Future reactors would likely use metallic electrodes, which should reduce low-Z impurity influx and allow the plasma intrinsic temperatures to be higher. In addition, as noted in Sec. III C, the loop voltage generated by the decaying plasma should heat the CHI plasma, and since much higher levels of startup flux would be employed in future devices, this heating could be substantial.

The Coppi-Tang L-mode transport model and a Spitzer resistivity model[29] were used. The L-mode density profile shape was prescribed, and has a peaking factor of approximately 1.1. The Z_{eff} value was specified as 3.0 and maintained constant in time and space. Simulations were conducted for three levels of flux injection into the NSTX vessel geometry at a toroidal field of 1 T. The magnitude of the toroidal field does not affect the magnitude of the attained closed flux current, but higher levels of the toroidal field simply help with reducing the injector current needed to inject a given amount of flux. Since the purpose here was to see the effect on the electron temperature as a function of injected flux magnitude, this was adequate for the present study. Injector flux values corresponding to 52 mWb, 104 mWb and 208 mWb are used.

The results of the study are shown in Fig. 5. Figure 5(a) shows the magnitude of the closed-flux plasma current I_p as a function of time. It quite clearly shows that the magnitude of I_p does indeed increase with the injected flux. At 30 ms, these plasmas contain plasma currents corresponding to about 100, 200, and 400 kA of the toroidal plasma current, respectively, for $\psi_{inj} = 52$ mWb, 104 mWb, and 208 mWb.

Figure 5(b) shows the Ohmic power input P_{self} due to the induced loop voltage. Early on, when the electron temperature T_e is low, this is quite substantial, reaching over 4 MW for the highest-flux case, similar to the values for the simple estimates in Sec. III C.

The Ohmic power input decreases in time as the plasma heats up, although the heating of the plasma, in turn, slows down the decay time. The resulting electron heating is shown in Fig. 5(c). The electron temperature increases substantially, reaching over 1 keV for the highest flux used in these simulations.

Figure 5(d) shows the normalized plasma internal inductance l_i, which is quite small at the CHI plasma formation time (about 0.1) and gradually increases to over 0.8 as the initially hollow current profile relaxes into a profile more typical of Ohmically heated plasmas.

In these simulations, no additional heating sources were incorporated. In reality, reactor devices would employ high-power heating sources, which would heat the plasma further and increase the current relaxation time. In addition, a combination of heating and current-drive sources would be used to maintain the required current profile. The details of current profile maintenance are beyond the scope of this study, which is primarily aimed at assessing the intrinsic electron temperature of transient CHI plasmas as the magnitude of the injector flux is substantially increased from those used in present experiments.

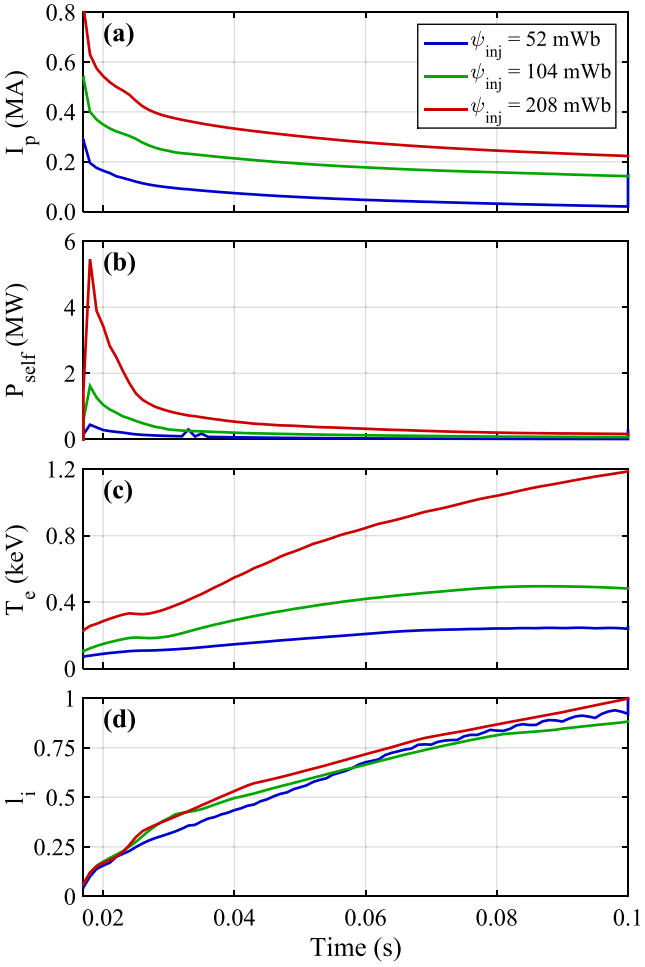

FIG. 5. Time traces of selected plasma parameters calculated in TSC simulations of CHI plasma evolution with different levels of injector flux.

V. CONCLUSIONS AND OUTLOOK

In this paper, simple models were employed to predict the required parameters for breaking down a plasma and attaining closed-flux currents of up to 1 MA using transient CHI in reactor-scale devices. Spatially resolved calculations of the minimum pressure required for breakdown indicated that the use of an NSTX-like electrode configuration could pose a high risk of failure due to breakdown in undesired locations; hence, it is strongly recommended to use toroidal ring electrodes which are localized to the divertor area. This also has the advantage of requiring simpler support for the insulators, as the insulators would not need to support large components as they would in the NSTX-like configuration.[18] Assuming the use of the latter electrode configuration, it is predicted that transient CHI start-up should be practicable in ST- and tokamak-like variants of a proposed ST-FNSF reactor, using at least 1 Wb of injector flux to attain MA-scale

plasma currents. The predictions assumed an optimistic scaling of transient CHI parameters with injector flux. These scaling predictions are supported by TSC simulations tracking CHI plasma evolution, which found strong increases in plasma current, self-heating power, and electron temperatures in response to increases in injector flux.

This study considered an existing design for a ST-FNSF reactor along with several possible modifications with higher aspect ratios, larger toroidal fields, and more spacing between the biasing electrodes. These modifications would all ease the requirements on some key parameters relevant to breakdown and CHI—namely, the gas pressure required for breakdown and the minimum injector current—although the impacts on the key output parameters of interest—plasma current and self-heating power—were not as dramatic. While a wider electrode gap would permit a substantially lower injector current, it should be noted that it may also reduce the efficiency with which the injector flux is coupled to closed poloidal flux.[8]

While the localized ring electrode concept appears to be a fundamental requirement for reactor-scale transient CHI experiments, most transient CHI work to date has not employed such electrodes. Fortunately, new and upcoming experiments will investigate a variety of ring electrode concepts in detail. The QUEST device has recently implemented a single ring electrode in the lower divertor area which is biased relative to the vessel wall.[24,30] Further transient CHI experiments are expected to begin on the URANIA device (formerly, PEGASUS) at the University of Wisconsin. URANIA will test a configuration with two independently biased electrodes, which will allow extra flexibility to optimize the breakdown and injection processes. In addition, both QUEST and URANIA will test the coupling of the transient CHI discharge to ECRH.

ACKNOWLEDGMENTS

This work was supported by the U.S. Department of Energy under Contract Nos. DE-FG02-99ER54519 and DE-AC02-09CH11466. The digital data for this paper may be found at http://arks.princeton.edu/ark:/88435/dsp011544br87z.

REFERENCES

[1]R. Raman and V. F. Shevchenko, Plasma Phys. Controlled Fusion **56**, 103001 (2014).
[2]J. Kim, W. Choe, and M. Ono, Plasma Phys. Controlled Fusion **46**, 1647 (2004).
[3]M. Ushigome, S. Ide, S. Itoh, E. Jotaki, O. Mitarai, S. Shiraiwa, T. Suzuki, Y. Takase, S. Tanaka, T. Fujita, P. Gohil, Y. Kamada, L. Lao, T. Luce, Y. Miura, O. Naito, T. Ozeki, P. Politzer, Y. Sakamoto, and JT-60 Team, Nucl. Fusion **46**, 207 (2006).
[4]Y. Takase, A. Ejiri, H. Kakuda, Y. Nagashima, T. Wakatsuki, O. Watanabe, P. Bonoli, O. Meneghini, S. Shiraiwa, J. Wright, C. Moeller, H. Kasahara, R. Kumazawa, T. Mutoh, K. Saito, and TST-2 Group, Nucl. Fusion **51**, 063017 (2011).
[5]M. Gryaznevich, V. Shevchenko, and A. Sykes, Nucl. Fusion **46**, S573 (2006).
[6]D. J. Battaglia, M. W. Bongard, R. J. Fonck, A. J. Redd, and A. C. Sontag, Phys. Rev. Lett. **102**, 225003 (2009).
[7]R. Raman, T. R. Jarboe, D. Mueller, M. J. Schaffer, R. Maqueda, B. A. Nelson, S. A. Sabbagh, R. Ewig, E. D. Fredrickson, D. A. Gates, J. C. Hosea, S. C. Jardin, H. Ji, R. Kaita, S. M. Kaye, H. W. Kugel, L. L. Lao, R. Maingi, J. Menard, M. Ono, D. Orvis, F. Paoletti, S. F. Paul, Y. K. M. Peng, C. H. Skinner, J. B. Wilgen, S. J. Zweben, and NSTX research Team, Nucl. Fusion **41**, 1081 (2001).
[8]F. Ebrahimi, R. Raman, E. B. Hooper, C. R. Sovinec, and A. Bhattacharjee, Phys. Plasmas **21**, 056109 (2014).
[9]F. Ebrahimi and R. Raman, Phys. Rev. Lett. **114**, 205003 (2015).
[10]F. Ebrahimi and R. Raman, Nucl. Fusion **56**, 044002 (2016).
[11]R. Raman, T. R. Jarboe, B. A. Nelson, V. A. Izzo, R. G. O'Neill, A. J. Redd, and R. J. Smith, Phys. Rev. Lett. **90**, 075005 (2003).
[12]R. Raman, B. A. Nelson, M. G. Bell, T. R. Jarboe, D. Mueller, T. Bigelow, B. LeBlanc, R. Maqueda, J. Menard, M. Ono, and R. Wilson, Phys. Rev. Lett. **97**, 175002 (2006).
[13]T. R. Jarboe, Fusion Technol. **15**, 7 (1989).
[14]A. von Engel, *Ionized Gases* (Clarendon Press, 1955).
[15]T. Brown, J. Menard, L. El Guebaly, and A. Davis, Fusion Sci. Technol. **68**, 277 (2015).
[16]R. Raman, T. R. Jarboe, R. G. O'Neill, W. T. Hamp, B. A. Nelson, V. A. Izzo, A. J. Redd, P. E. Sieck, and R. J. Smith, Nucl. Fusion **45**, L15 (2005).
[17]M. J. Schaffer, M. Ali Mahdavi, C. C. Klepper, D. N. Hill, and M. E. Rensink, Nucl. Fusion **32**, 855 (1992).
[18]R. Raman, T. Brown, L. A. El Guebaly, T. R. Jarboe, B. A. Nelson, and J. E. Menard, Fusion Sci. Technol. **68**, 674 (2015).
[19]K. C. Hammond, R. Raman, and F. A. Volpe, Nucl. Fusion **58**, 016013 (2018).
[20]D. J. Rose, Phys. Rev. **104**, 273 (1956).
[21]B. Lloyd, G. Jackson, T. Taylor, E. Lazarus, T. Luce, and R. Prater, Nucl. Fusion **31**, 2031 (1991).
[22]R. Yoshino and M. Seki, Plasma Phys. Controlled Fusion **39**, 205 (1997).
[23]P. de Vries, A. Sips, H. Kim, P. Lomas, F. Maviglia, R. Albanese, I. Coffey, E. Joffrin, M. Lehnen, A. Manzanares, M. O'Mulane, I. Nunes, G. van Rooij, F. Rimini, M. Stamp, and JET-EFDA Contributors, Nucl. Fusion **53**, 053003 (2013).
[24]K. Kuroda, R. Raman, K. Hanada, M. Hasegawa, T. Onchi, M. Ono, B. A. Nelson, T. R. Jarboe, M. Nagata, O. Mitarai, K. Nakamura, H. Idei, J. Rogers, S. Kawasaki, T. Nagata, A. Kuzmin, S. Kojima, C. Huang, O. Watanabe, A. Higashijima, Y. Takase, A. Fukuyama, and S. Murakami, Plasma Phys. Controlled Fusion **60**, 115001 (2018).
[25]R. J. Armstrong and T. K. Bennett, J. Appl. Phys. **82**, 2147 (1997).
[26]R. Raman, S. C. Jardin, J. Menard, T. R. Jarboe, M. Bell, D. Mueller, B. A. Nelson, and M. Ono, Nucl. Fusion **51**, 113018 (2011).
[27]R. Raman, D. Mueller, T. R. Jarboe, B. A. Nelson, M. G. Bell, S. Gerhardt, B. LeBlanc, J. Menard, M. Ono, L. Roquemore, and V. Soukhanovskii, Phys. Plasmas **18**, 092504 (2011).
[28]S. C. Jardin, N. Pomphrey, and J. DeLucia, J. Comput. Phys. **66**, 481 (1986).
[29]S. C. Jardin, M. G. Bell, and N. Pomphrey, Nucl. Fusion **33**, 371 (1993).
[30]K. Kuroda, R. Raman, K. Hanada, M. Hasegawa, T. Onchi, M. Ono, T. Jarboe, B. A. Nelson, M. Nagata, O. Mitarai, K. Nakamura, H. Idei, J. Rogers, S. Kawasaki, T. Nagata, A. Kuzmin, S. Kojima, O. Watanabe, A. Higashijima, Y. Takase, and A. Fukuyama, Plasma Fusion Res.: Rapid Commun. **12**, 1202020 (2017).
[31]L. L. Lao, H. St. John, R. D. Stambaugh, A. G. Kellman, and W. Pfeiffer, Nucl. Fusion **25**, 1611 (1985).